Journal of Solid State Chemistry 184 (2011) 149–153

Contents lists available at ScienceDirect

Journal of Solid State Chemistry

journal homepage: www.elsevier.com/locate/jssc

The crystal structure of π-$ErBO_3$: New single-crystal data for an old problem ☆

Almut Pitscheider [a], Reinhard Kaindl [b], Oliver Oeckler [c], Hubert Huppertz [a,*]

[a] Institut für Allgemeine, Anorganische und Theoretische Chemie, Leopold-Franzens-Universität Innsbruck, Innrain 52a, A-6020 Innsbruck, Austria
[b] Institut für Mineralogie und Petrographie, Leopold-Franzens-Universität Innsbruck, Innrain 52, A-6020 Innsbruck, Austria
[c] Department Chemie, Ludwig-Maximilians-Universität München, Butenandtstrasse 5–13, D-81377 München, Germany

ARTICLE INFO

Article history:
Received 24 September 2010
Received in revised form
8 November 2010
Accepted 9 November 2010
Available online 13 November 2010

Keywords:
Rare-earth
Orthoborate
High-pressure
Crystal structure

ABSTRACT

Single crystals of the orthoborate π-$ErBO_3$ were synthesized from Er_2O_3 and B_2O_3 under high-pressure/high-temperature conditions of 2 GPa and 800 °C in a Walker-type multianvil apparatus. The crystal structure was determined on the basis of single-crystal X-ray diffraction data, collected at room temperature. The title compound crystallizes in the monoclinic pseudowollastonite-type structure, space group $C2/c$, with the lattice parameters $a=1128.4(2)$ pm, $b=652.6(2)$ pm, $c=954.0(2)$ pm, and $\beta=112.8(1)°$ ($R_1=0.0124$ and $wR_2=0.0404$ for all data).

1. Introduction

The rare-earth orthoborates $RE BO_3$ are of great scientific interest, due to their extraordinary optical properties like vacuum ultraviolet (VUV) transparency, outstanding optical damage threshold, and high luminescent efficiencies for Eu^{3+}-doped orthoborates. These compounds are thus attractive materials to be used in vacuum discharge lamps or screens and numerous studies have been performed on these borates in the past decades. The rare-earth orthoborates $RE BO_3$ exhibit a complex polymorphism and most of them are designated with Greek letters according to the nomenclature of Meyer [1–3]. An overview of the known phases is given in Table 1.

While the crystal structures of most polymorphs have been determined unambiguously, there are a low-temperature modification and a high-temperature modification termed π-$RE BO_3$ (RE=Y, Nd, Sm–Lu) and μ-$RE BO_3$ (RE=Y, Sm–Gd, Dy–Lu), respectively, which are still the objects of lengthy discussions in the literature. In the following, a survey of the previous works is given:

(a) In 1961, Levin et al. [4] first described the orthoborates π-$RE BO_3$ (RE=Y, Nd, Sm–Lu) as pseudo-hexagonal vaterite-type borates with a possible boron coordination of more than three. A phase transition into μ-$RE BO_3$ was observed, which was proposed to be nearly isostructural with vaterite, but also possibly pseudohexagonal.

(b) Newnham et al. [22] presented the first structure determination of π-YBO_3 powder in 1963 and proposed two possible hexagonal structure models with BO_3-groups. One was a disordered model with space group $P6_3/mmc$, the other one an ordered model with space group $P6_3/mcm$. Each rare-earth ion was said to be coordinated to eight oxygen atoms arranged in a distorted cube.

(c) In the following years, several IR, NMR, and Raman studies were performed on the π-orthoborates, all indicating a tetrahedral boron coordination in the form of B_3O_9-rings [29–33]. Bradley et al. [23] thus presented in 1966 the first structure determination from X-ray powder data, that accommodated these findings. For the low-temperature form π-$RE BO_3$, the hexagonal space group $P\bar{6}c2$ was reported, based on Newnham's disordered model. Either a triangular boron coordination, analogous with vaterite, or a three-membered ring of boron tetrahedra were considered to be possible. For the high-temperature form μ-$RE BO_3$, the hexagonal space group $P6_322$ with tilted triangular anions was derived.

(d) In 1977, Morgan et al. [24] picked up the thought of pseudo-hexagonality for the π-orthoborates, as indicated in the very beginning by Levin et al. Based on Bradley's model, they calculated a model in the monoclinic space group $C2/c$ with a pseudohexagonal stacking of the B_3O_9-rings. The compounds were assumed to crystallize in a pseudowollastonite-type structure rather than in a vaterite-type one.

(e) It was not until 1997, when the first single-crystal structure for π-YBO_3 was reported by Chadeyron et al. [25]. Here, the structure was solved in the hexagonal space group $P6_3/m$. The model implies the partial occupation of oxygen and boron

☆ Dedicated to Professor Peter Klüfers on the occasion of his 60th birthday.

* Corresponding author.
E-mail address: Hubert.Huppertz@uibk.ac.at (H. Huppertz).

0022-4596/$ - see front matter © 2010 Elsevier Inc. All rights reserved.
doi:10.1016/j.jssc.2010.11.018

Table 1
Known polymorphs of $RE BO_3$.

Polymorphs	*RE*	Comments
β-$RE BO_3$	Sc, Er–Lu	Calcite structure [3–9]
λ-$RE BO_3$	La–Nd, Sm, Eu	Aragonite structure [4,10–12]
χ-$RE BO_3$	Dy–Er	Triclinic phases [13,14]
ν-$RE BO_3$	Ce–Nd, Sm–Dy	Triclinic (H–$NdBO_3$) [2,15–18]
H–$RE BO_3$	La, Ce, Nd	Monoclinic (H–$LaBO_3$) [19–21]
π-$RE BO_3$	Y, Nd, Sm–Lu	Low-temperature phases [4,9,22–28]
μ-$RE BO_3$	Y, Sm–Gd, Dy–Lu	High-temperature phases [3,23,26–28]

atoms and a possible rotational distortion of the B_3O_9-rings. BO_4-tetrahedra were identified at least as the main structural unit *via* IR and NMR investigations.

(f) Two years later, Ren et al. [26] brought two other space groups for π- and μ-$RE BO_3$ into the discussion. On the basis of powder diffraction data, Chadeyron's hexagonal cell of π-YBO_3 was identified as a subcell of a rhombohedral structure. This way, a fully ordered structure in the rhombohedral space group *R*32 for π-$RE BO_3$ was obtained, but unreasonable bond distances gave rise to doubts. The high-temperature polymorph μ-$RE BO_3$ was said to crystallize in $P6_3/mmc$, the hexagonal space group previously identified for the low-temperature form by Newnham et al.

(g) Powder data of π-$GdBO_3$ from Cohen-Adad et al. [27] in 2000 were consistent with all proposed hexagonal space groups $P6_3/mmc$, $P\bar{6}c2$, $P6_3/mcm$, and $P6_3/m$, while the best agreement could be accounted in $P\bar{6}c2$. For μ-$GdBO_3$, the hexagonal space group $P6_322$ was assumed; both models are in agreement with the earlier findings of Bradley et al.

(h) A neutron diffraction study on $(Y_{0.92}Er_{0.08})BO_3$ powder samples was undertaken by Lin et al. [28] in 2004. The powder diffraction patterns of both the π- and the μ-orthoborate could only be indexed assuming a monoclinic cell in the space group $C2/c$, and the results thus support the earlier structure determination of Morgan et al. This monoclinic lattice was related to the rhombohedral lattice, observed by Ren et al. by removing the 3-fold axis.

(i) In 2008, Hosokawa et al. [9] presented another study on orthoborate powders synthesized by a glycothermal reaction. Here, the space group $P6_3/m$ was reported as previously determined from single-crystal data by Chadeyron et al.

It is clear from the literature that the crystal structure of the π- and the μ-orthoborate has to be clarified. The red $(Y,Gd)BO_3:Eu^{3+}$ phosphor is known to be one of the most familiar materials, being used for plasma panel displays, and its luminescent properties are often discussed on the basis of a hexagonal vaterite-type structure. Looking at the above-mentioned studies, this cannot be taken for granted. Because of its importance in application, it is highly desirable to refine this structure satisfactorily. Over the past 50 years, five different structural models were proposed, revised, doubted, and supported. Remarkably, only one single-crystal measurement on π-YBO_3 was reported, while all other models are based on powder measurements. Light pressure during solid state syntheses often yields coarse-crystalline samples of the products, due to pressure-induced crystallization [34]. The high-pressure/high-temperature synthesis now resulted in single crystals of π-$ErBO_3$, which made the first satisfying single-crystal structure determination possible.

2. Experimental section

2.1. Synthesis

A 1:1 mixture of Er_2O_3 (Strem Chemicals, 99.9%) and B_2O_3 (Strem Chemicals, 99.9+%) was ground and filled into a boron nitride crucible (Henze BNP GmbH, HeBoSint®S100, Kempten, Germany). This crucible was placed into the center of an 18/11-assembly, which was compressed by eight tungsten carbide cubes (TSM-10 Ceratizit, Reutte, Austria). The details of preparing the assembly can be found in Refs. [35–39]. Pressure was applied by a multianvil device, based on a Walker-type module and a 1000 ton press (both devices from the company Voggenreiter, Mainleus, Germany). The sample was compressed up to 2 GPa in 75 min, then heated to 800 °C in 10 min and kept there for 20 min. Afterwards, the sample was cooled down to 600 °C in 20 min and then to room temperature by switching off the heating. The decompression of the assembly required 3.75 h. The recovered MgO-octahedron (pressure transmitting medium, Ceramic Substrates & Components Ltd., Newport, Isle of Wight, UK) was broken apart revealing nearly phase pure π-$ErBO_3$, from which pink air- and water-resistant crystal platelets were obtained for the single-crystal structure determination.

2.2. Crystal structure analysis

The intensity data of a single-crystal of π-$ErBO_3$ were collected at room temperature, using a Nonius Kappa-CCD diffractometer with graded multilayer X-ray optics (Mo$K\alpha$ radiation, $\lambda = 71.073$ pm). Afterwards, a multi-scan absorption correction was applied to the data [40]. All relevant details of the data collection and evaluation are listed in Table 2. According to the systematic extinctions, the monoclinic space groups *Cc* and *C*2/*c* were derived. Structure solution and parameter refinement (full-matrix least-squares against F^2) were performed successfully in the space group *C*2/*c*, using the SHELX–97 software suite [41] with anisotropic atomic displacement parameters for all atoms. The positional parameters, interatomic distances, and interatomic angles are listed in Tables 3 and 4.

Further information of the crystal structure is available from the Fachinformationszentrum Karlsruhe (crysdata@fiz-karlsruhe.de), D-76344 Eggenstein-Leopoldshafen (Germany), quoting the Registry no. CSD-422094.

Table 2
Crystal data and structure refinement for π-$ErBO_3$.

Empirical formula	$ErBO_3$
Molar mass, g mol^{-1}	226.07
Crystal system	Monoclinic
Space group	*C*2/*c* (No. 15)
Single-crystal diffractometer	Bruker AXS/Nonius Kappa CCD
Radiation	Mo$K\alpha$ ($\lambda = 71.073$ pm) (graphite monochromator)
a, pm	1128.4(2)
b, pm	652.6(2)
c, pm	954.0(2)
β, deg.	112.8(1)
Volume, nm^3	0.6476(2)
Formula units per cell	$Z = 12$
Temperature, K	293(2)
Calculated density, g cm^{-3}	6.96
Crystal size, mm^3	$0.04 \times 0.04 \times 0.02$
Absorption coefficient, mm^{-1}	38.5
$F(0\,0\,0)$, e	1164
θ range, deg.	3.7–30.0
Range in *hkl*	± 15, ± 9, ± 13
Total number of reflections	3552
Independent reflections/R_{int}	946/0.0202
Reflections with $I \geq 2\sigma(I)/R_\sigma$	914/0.0170
Data/ref. parameters	946/72
Absorption correction	semiempirical [40]
Goodness-of-fit on F^2	1.016
Final indices R_1/wR_2 [$I \geq 2\sigma(I)$]	0.0120/0.0401
Indices R_1/wR_2 (all data)	0.0124/0.0404
Larg. diff. peak/hole, e Å^{-3}	1.06/−0.77

2.3. IR spectroscopy

FTIR-attenuated total reflection (ATR) spectra of the crystals were recorded with a Bruker Vertex 70 FT-IR spectrometer (resolution ~0.5 cm^{-1}), attached to a Hyperion 3000 microscope in a spectral range from 600–4000 cm^{-1}. A frustrum shaped germanium ATR-crystal with a tip diameter of 100 μm was pressed on the surface of the crystals with a power of 5 N, which let them crush into pieces of μm-size. Sixty-four scans for sample and background were acquired. Beside spectra correction for atmospheric influences, an enhanced ATR-correction, [42] using the OPUS 6.5 software, was performed. A mean refraction index of the sample of 1.6 was assumed for the ATR-correction.

2.4. Raman spectroscopy

Confocal Raman spectra of single crystals were gained with a HORIBA JOBIN YVON LabRam-HR 800 Raman micro-spectrometer. The sample was excited, using the 633 nm emission line of a 17 mW He–Ne–laser and an OLYMPUS 100 × objective (numerical aperture = 0.9). The size and power of the laser spot on the surface were approximately 1 μm and 5 mW, respectively. The scattered light was dispersed by a grating with 1800 lines/mm and collected by a 1024 × 256 open electrode CCD detector. The spectral resolution, determined by measuring the Rayleigh line, was about 1.4 cm^{-1}. The wavenumber accuracy of about 0.5 cm^{-1} was achieved by adjusting the zero-order position of the grating and regularly checked by a Neon spectral calibration lamp.

3. Results and discussion

The single-crystal structure of π-$ErBO_3$ could be solved and refined in the space group *C*2/*c* and is thus isotypic to the pseudowollastonite-type $CaSiO_3$ [43] and not to the vaterite-type $CaCO_3$ [44]. The results agree with the findings of Morgan et al. [24] and the neutron diffraction study of Lin et al. [28]. From the single-crystal data, we unambiguously derived a monoclinic unit cell with the parameters *a* = 1128.4(2) pm, *b* = 652.6(2) pm, *c* = 954.0(2) pm,

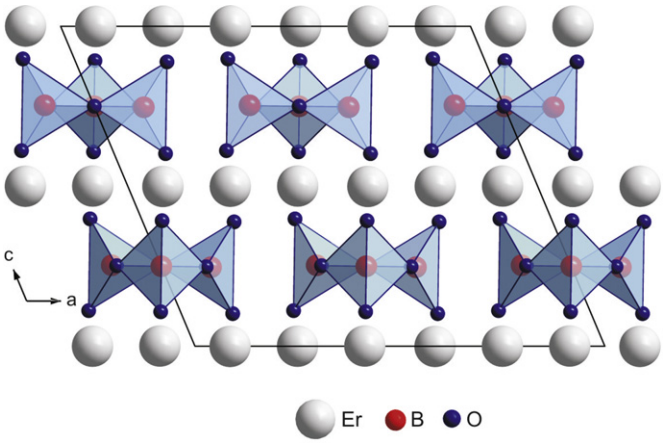

Fig. 1. Crystal structure of π-$ErBO_3$ along [0 1 0], displaying isolated B_3O_9-rings of BO_4-tetrahedra.

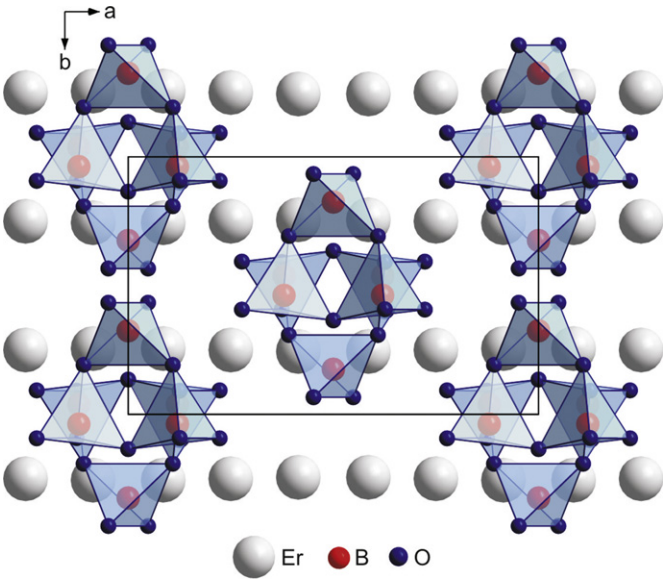

Fig. 2. Crystal structure of π-$ErBO_3$ along [0 0 1], displaying the staggered stacking of the B_3O_9-rings.

Table 3
Atomic coordinates and isotropic equivalent displacement parameters U_{eq} ($Å^2$) for π-$ErBO_3$ (space group *C*2/*c*).

Atom	*Wyckoff* position	*x*	*y*	*z*	U_{eq}
Er1	4*c*	1/4	1/4	0	0.00399(7)
Er2	8*f*	0.085415(7)	0.25566(2)	0.499356(7)	0.00376(7)
B1	8*f*	0.1201(2)	0.0379(3)	0.2469(2)	0.0058(3)
B2	4*e*	0	0.6752(4)	1/4	0.0057(4)
O1	8*f*	0.1255(2)	0.0920(2)	0.1020(2)	0.0062(2)
O2	8*f*	0.2229(2)	0.0932(2)	0.3887(2)	0.0061(2)
O3	8*f*	0.0484(2)	0.5664(2)	0.3923(2)	0.0061(2)
O4	8*f*	0.3914(2)	0.3082(2)	0.2517(2)	0.0056(2)
O5	4*e*	0	0.1350(2)	1/4	0.0052(3)

U_{eq} is defined as one third of the trace of the orthogonalized U_{ij} tensor.

Table 4
Interatomic distances (pm) and angles (deg.), calculated with the single-crystal lattice parameters of π-$ErBO_3$ with standard deviations in parentheses.

Er1–O1	224.6(2)	Er2–O3	223.6(2)	B1–O2	144.5(2)	B2–O3	143.9(2)
	2 ×	Er2–O2	223.6(2)	B1–O1	145.1(2)		2 ×
Er1–O4	234.3(2)	Er2–O4	232.4(2)	B1–O4	150.5(2)	B2–O4	150.7(2)
	2 ×	Er2–O5	233.0(2)	B1–O5	150.7(2)		2 ×
Er1–O3	242.0(2)	Er2–O3	243.0(2)		**Ø = 147.7**		**Ø = 147.3**
	2 ×	Er2–O2	243.3(2)				
Er1–O2	244.6(2)	Er2–O1	244.1(2)	O2–B1–O1	121.1(2)	O3–B2–O3	120.9(2)
	2 ×	Er2–O1	244.3(2)	O2–B1–O4	106.3(2)	O3–B2–O4	106.4(2)
	Ø = 236.4		**Ø = 235.9**	O1–B1–O4	106.6(2)		2 ×
				O2–B1–O5	106.2(2)	O3–B2–O4	106.6(2)
				O1–B1–O5	106.7(2)		2 ×
				O4–B1–O5	109.7(2)	O4–B2–O4	109.6(2)

and $\beta = 112.8(1)^\circ$ (Table 2). The parameters of the neutron powder diffraction experiments are similar with $a = 1131.38(3)$ pm, $b = 654.03(2)$ pm, $c = 954.99(2)$ pm, and $\beta = 112.902(1)^\circ$ [28], while no cell parameters were given by Morgan et al.

The crystal structure of π-$ErBO_3$ has got two crystallographically independent boron cations (Table 3), which are fourfold coordinated by oxygen anions. Connecting *via* common corners, three BO_4-tetrahedra (two around B1 and one around B2) form isolated B_3O_9-rings (Fig. 1). The tetrahedra are regular with a displacement of the central boron atoms towards the non-bridging oxygen atoms, resulting in two shorter and two larger B–O bonds for each boron atom (Table 4). A similar distortion for BO_4-tetrahedra with two bridging and two non-bridging ligands was observed previously, *e.g.* in the fluoride borate $La_4B_4O_{11}F_2$ [45]. With an average B–O bond lengths of 147.7 and 147.3 pm, they go together with the known average value of 147.6 pm for BO_4-tetrahedra in borates [46,47]. The bond lengths are comparable, but more consistent than those obtained by Lin et al. *via* powder neutron diffraction [28]. For one of the hexagonal structure models, Chadeyron et al. report B–O bond lengths between 137 and 192 pm [25], which are rather doubtful for BO_4-tetrahedra. The distortions of the BO_4-tetrahedra in π-$ErBO_3$ also cause enlarged O–B–O angles of $\sim 120^\circ$ between the non-bridging oxygen atoms.

Viewing along [0 0 1], the B_3O_9-rings are stacked in a shifted arrangement (Fig. 2). Earlier structure determinations assumed the presence of rare-earth cations inside of the B_3O_9-rings [23], which can be now excluded from the single-crystal structure determination. Due to the staggered arrangement and the distortion of the BO_4-tetrahedra, three- or sixfold rotational axes do not exist in the structure of π-$ErBO_3$. Therefore, all hexagonal and rhombohedral models have to take disorder or partially occupied atomic positions into account, which is not the case for the monoclinic model, stated earlier by Lin et al. [28].

The two erbium cations in the structure are both eightfold coordinated (Fig. 3). The Er–O distances are in a narrow range between 223.6(2) and 244.6(2) pm. They are thus much more uniformly distributed than the bond lengths reported for π-YBO_3 by Lin et al., which range between 225.7(8)–295.0(8) pm [28].

The calculations of the bond-valence sums for π-$ErBO_3$ with the bond-length/bond-strength (BLBS) concept [48] and the charge distribution concept (CHARDI) in solids according to Hoppe [49–51] were performed and confirmed the formal ionic charges of the single-crystal structure analysis (Table 5).

Furthermore, we calculated the Madelung Part of Lattice Energy value (MAPLE) according to Hoppe [52–54] of π-$ErBO_3$ in order to compare it with the sum of the MAPLE values for the high-pressure modification of Er_2O_3 [55] and that of B_2O_3-II [56] [0.5 Er_2O_3 (15,283 kJ mol^{-1})+0.5 B_2O_3-II (21,938 kJ mol^{-1})]. The calculated value (18,739 kJ mol^{-1}) for π-$ErBO_3$ and the MAPLE value of the sum of the binary oxides (18,611 kJ mol^{-1}) tally well (deviation 0.7%).

Fig. 4 shows the FTIR-ATR measurement of the sample between 600 and 2000 cm^{-1}. The main absorption bands between 750 and 1250 cm^{-1} are those typical for the tetrahedral borate group $[BO_4]^{5-}$ as in π-$GdBO_3$, π-YBO_3, or $TaBO_4$ [26,31,57]. Fig. 5 shows the Raman spectrum of π-$ErBO_3$ in the range 100–1500 cm^{-1}. In previous Raman measurements of borates, the area below 650 cm^{-1} could be assigned to lattice and *RE*–O modes. Therefore, the area between 700 and 1100 cm^{-1} shows probably the bands evoked by the BO_4-groups. The positions of these Raman bands (Fig. 5) are compared to those reported for π-$GdBO_3$ in the literature (Table 6) [27] .

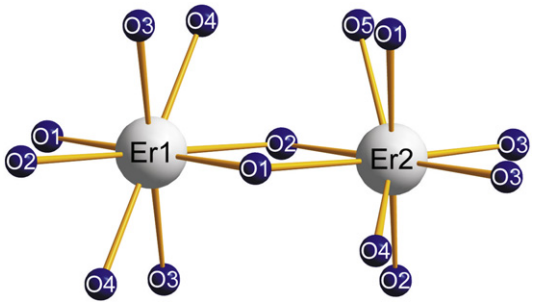

Fig. 3. Coordination spheres of the erbium cations in the crystal structure of π-$ErBO_3$.

Table 5
Charge distribution in π-$ErBO_3$, calculated with VaList (ΣV) and the CHARDI concept (ΣQ).

	Er1	Er2	B1	B2	O1	O2	O3	O4	O5
ΣV	+2.97	+3.01	+3.01	+3.05	−1.89	−1.92	−1.96	−2.18	−2.18
ΣQ	+3.03	+3.02	+2.99	+2.95	−1.91	−1.94	−1.98	−2.11	−2.12

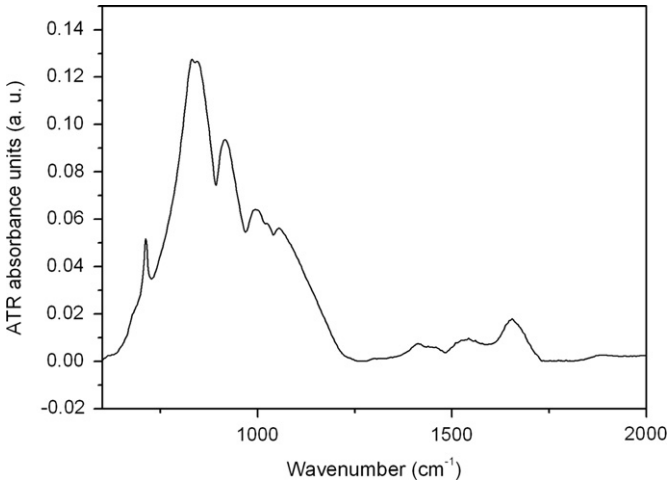

Fig. 4. FTIR-ATR spectrum of π-$ErBO_3$ in the range 600–2000 cm^{-1}.

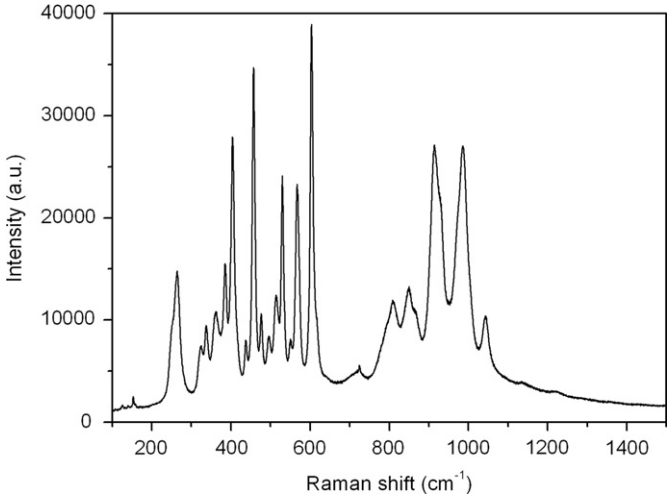

Fig. 5. Raman spectrum of π-$ErBO_3$ in the range 100–1500 cm^{-1}.

Table 6
Wavenumbers of Raman bands in the spectrum of π-$ErBO_3$ single crystals (left) and of bands of π-$GdBO_3$, reported for the bulk material (right) [27].

Single-crystal Raman bands (π-$ErBO_3$)	Bulk Raman bands (π-$GdBO_3$)
724	
810	825
849	843
865	881
913	918
986	996
1043	1016

4. Conclusions

In this paper, we presented the first satisfying single-crystal structure determination of π-$ErBO_3$, which sheds additional light on the extensively discussed structure of π-orthoborates. The application of light pressure (2 GPa) during the solid state synthesis yielded a coarse-crystalline sample of this ambient-pressure phase, due to the pressure-induced crystallization. Based on the single-crystal data, we can support the monoclinic structural model, introduced by Morgan et al. [24] and Lin et al. [28]. Due to the staggered arrangement and the distortion of the BO_4-tetrahedra, no three- or sixfold rotational axes can be applied to the structure of π-$ErBO_3$. All hexagonal and rhombohedral models have to take disorder or partially occupied atomic positions into account, thus representing subcells and/or incorrectly averaged structural models. The neglecting of several very weak reflections and the splitting of appearing single reflections in the powder pattern led to numerous hexagonal cells. The new single-crystal data should end the discussion about the correct indexing of the powder patterns. The luminescence properties for the red $(Y,Gd)BO_3:Eu^{3+}$ phosphor should be discussed on the basis of a monoclinic rather than a hexagonal structure.

For the future, single crystals of the high-temperature polymorph μ-$REBO_3$ will be of great interest.

Appendix A. Supplementary materials

Supplementary data associated with this article can be found in the online version at doi:10.1016/j.jssc.2010.11.018.

References

[1] H.J. Meyer, Naturwissenschaften 56 (1969) 458.
[2] H.J. Meyer, Naturwissenschaften 59 (1972) 215.
[3] H.J. Meyer, A. Skokan, Naturwissenschaften 58 (1971) 566.
[4] E.M. Levin, R.S. Roth, J.B. Martin, Am. Mineral. 46 (1961) 1030.
[5] S.C. Abrahams, J.L. Bernstein, E.T. Keve, J. Appl. Crystallogr. 4 (1971) 284.
[6] T.A. Bither, H.S. Young, J. Solid State Chem. 6 (1973) 502.
[7] D.A. Keszler, H. Sun, Acta Crystallogr. C 44 (1988) 1505.
[8] H. Huppertz, Z. Naturforsch. 56b (2001) 697.
[9] S. Hosokawa, Y. Tanaka, S. Iwamoto, M. Inoue, J. Mater. Sci. 43 (2008) 2276.
[10] J. Weidelt, H.U. Bambauer, Naturwissenschaften 55 (1968) 342.
[11] G.K. Abdullaev, Kh.S. Mamedov, G.G. Dzhafarov, Azerb. Khim. Zh. (1976) 117.
[12] H. Müller-Bunz, T. Nikelski, Th. Schleid, Z. Naturforsch. 58b (2003) 375.
[13] H. Huppertz, B. von der Eltz, R.-D. Hoffmann, H. Piotrowski, J. Solid State Chem. 166 (2002) 203.
[14] H. Huppertz, Unpublished results.
[15] K.K. Palkina, V.G. Kuznetsov, L.A. Butman, B.F. Dzhurinskii, Acad. Sci. USSR 2 (1976) 286.
[16] G. Corbel, M. Leblanc, E. Antic-Fidancev, M. Lemaître-Blaise, J.C. Krupa, J. Alloys Compd. 287 (1999) 71.
[17] H. Emme, H. Huppertz, Acta Crystallogr. C 60 (2004) i117.
[18] S. Noirault, O. Joubert, M.T. Caldes, Y. Piffard, Acta Crystallogr. E 62 (2006) i228.
[19] R. Böhlhoff, H.U. Bambauer, W. Hoffmann, Naturwissenschaften 57 (1970) 129.
[20] R. Böhlhoff, H.U. Bambauer, W. Hoffmann, Z. Kristallogr. 133 (1971) 386.
[21] S. Lemanceau, G. Bertrand-Chadeyron, R. Mahiou, M. El-Ghozzi, J.C. Cousseins, P. Conflant, R.N. Vannier, J. Solid State Chem. 148 (1999) 229.
[22] R.E. Newnham, M.J. Redman, R.P. Santoro, J. Am. Ceram. Soc. 46 (1963) 253.
[23] W.F. Bradley, D.L. Graf, R.S. Roth, Acta Crystallogr. 20 (1966) 283.
[24] P.E.D. Morgan, P.J. Carroll, F.F. Lange, Mater. Res. Bull. 12 (1977) 251.
[25] G. Chadeyron, M. El-Ghozzi, R. Mahiou, A. Arbus, J.C. Cousseins, J. Solid State Chem. 128 (1997) 261.
[26] M. Ren, J.H. Lin, Y. Dong, L.Q. Yang, M.Z. Su, L.P. You, Chem. Mater. 11 (1999) 1576.
[27] M.Th. Cohen-Adad, Ch. Kappenstein, O. Aloui-Lebbou, C. Goutaudier, G. Panczer, C. Dujardin, C. Pedrini, P. Florian, D. Massiot, F. Gerard, J. Solid State Chem. 154 (2000) 204.
[28] J.H. Lin, S. Sheptyakov, Y. Wang, P. Allenspach, Chem. Mater. 16 (2004) 2418.
[29] C.E. Weir, E.R. Lippincott, J. Res. Natl. Bur. Stand. A 65 (1961) 173.
[30] C.E. Weir, R.A. Schroeder, J. Res. Natl. Bur. Stand. A 68 (1964) 465.
[31] J.P. Laperches, P. Tarte, Spectrochim. Acta 22 (1966) 1201.
[32] H.M. Kriz, P.J. Bray, J. Chem. Phys. 51 (1969) 3642.
[33] J.H. Denning, S.D. Ross, Spectrochim. Acta A 28 (1972) 1775.
[34] H. Huppertz, Chem. Commun. (2011) 10.1039/C0CC02715D.
[35] D. Walker, M.A. Carpenter, C.M. Hitch, Am. Mineral. 75 (1990) 1020.
[36] D. Walker, Am. Mineral. 76 (1991) 1092.
[37] H. Huppertz, Z. Kristallogr. 219 (2004) 330.
[38] D.C. Rubie, Phase Transitions 68 (1999) 431.
[39] N. Kawai, S. Endo, Rev. Sci. Instrum. 8 (1970) 1178.
[40] Z. Otwinowski, W. Minor, Methods Enzymol. 276 (1997) 307.
[41] G.M. Sheldrick, Acta Crystallogr. A 64 (2008) 112.
[42] F.M. Mirabella Jr. (Ed.), Principles, Theory, and Practice of Internal Reflection Spectroscopy in Internal Reflection Spectroscopy, Theory and Applications, Marcel Dekker Inc., New York, 1993, pp. 17–53.
[43] H. Yang, C.T. Prewitt, Am. Mineral. 84 (1999) 929.
[44] H.J. Meyer, Z. Kristallogr. 128 (1969) 183.
[45] A. Haberer, R. Kaindl, O. Oeckler, H. Huppertz, J. Solid State Chem. 183 (2010) 1970.
[46] F.C. Hawthorne, P.C. Burns, J.D. Grice, Reviews in Mineralogy (Chapter 2), in: Boron: Mineralogy, Petrology, and Geochemistry, vol. 33, Mineralogical Society of America, Washington, DC (1996).
[47] E. Zobetz, Z. Kristallogr. 191 (1990) 45.
[48] A.S. Wills, VaList Version 3.0.13, University College London, UK, 1998–2008 Program available from ⟨www.ccp14.ac.uk⟩.
[49] R. Hoppe, S. Voigt, H. Glaum, J. Kissel, H.P. Müller, K.J. Bernet, J. Less-Common Met. 156 (1989) 105.
[50] I.D. Brown, D. Altermatt, Acta Crystallogr. B 41 (1985) 244.
[51] N.E. Brese, M. O'Keeffe, Acta Crystallogr. B 47 (1991) 192.
[52] R. Hoppe, Angew. Chem. 78 (1966) 52;
R. Hoppe, Angew. Chem. Int. Ed. 5 (1966) 96.
[53] R. Hoppe, Angew. Chem. 82 (1970) 7;
R. Hoppe, Angew. Chem. Int. Ed. 9 (1970) 25.
[54] R. Hübenthal, M. Serafin, R. Hoppe, Maple (version 4.0), Program for the Calculation of Distances, Angles, Effective Coordination Numbers, Coordination Spheres, and Lattice Energies, University of Gießen, Gießen (Germany), (1993).
[55] H.R. Hoekstra, Inorg. Chem. 5 (1966) 754.
[56] C.T. Prewitt, R.D. Shannon, Acta Crystallogr. B 24 (1968) 869.
[57] G. Blasse, G.P.M. van den Heuvel, Phys. Status Solidi 19 (1973) 111.